

# Foucault test: shadowgram modeling from the physical theory for quantitative evaluations

Jesús Villa,<sup>1,\*</sup> Gustavo Rodríguez,<sup>1</sup> Ismael de la Rosa,<sup>1</sup> Rumen Ivanov,<sup>2</sup>  
Tonatiuh Saucedo,<sup>2</sup> and Efrén González<sup>1</sup>

<sup>1</sup>Unidad Académica de Ingeniería Eléctrica, Universidad Autónoma de Zacatecas, Av. Ramón López Velarde 801, Zacatecas 98000, Mexico

<sup>2</sup>Unidad Académica de Física, Universidad Autónoma de Zacatecas, Calz. Solidaridad, Esquina Paseo de la Bufa s/n, Zacatecas 98060, Mexico

\*Corresponding author: [jvillah@uaz.edu.mx](mailto:jvillah@uaz.edu.mx)

Received August 19, 2014; revised October 16, 2014; accepted October 27, 2014;  
posted November 4, 2014 (Doc. ID 221284); published November 17, 2014

The physical theory of the Foucault test has been investigated to represent the complex amplitude and irradiance of the shadowgram in terms of the wavefront error; however, most of the studies have limited the treatment for the particular case of nearly diffraction-limited optical devices (i.e., aberrations smaller than the wavelength). In this paper we discard this restriction, and in order to show a more precise interpretation from the physical theory we derive expressions for the complex amplitude and the irradiance over an optical device with larger aberrations. To the best of our knowledge, it is the first time an expression is obtained in closed form. As will be seen, the result of this derivation is obtained using some properties of the Hilbert transform that permit representing the irradiance in a simple form in terms of the partial derivatives of the wavefront error. Additionally, we briefly describe from this point of view a methodology for the quantitative analysis of the test. © 2014 Optical Society of America

OCIS codes: (120.4800) Optical standards and testing; (120.3180) Interferometry.

<http://dx.doi.org/10.1364/JOSAA.31.002719>

## 1. INTRODUCTION

As a Schlieren technique the Foucault test is very simple, highly sensitive, and very useful for testing optical devices, such as lenses and mirrors. The Foucault test has been widely applied over several decades to assess the quality of telescope mirrors by means of detecting transverse aberrations using a simple knife edge that blocks out part of the rays to form a shadow pattern, usually called shadowgram. Despite its advantages, the Foucault test has been mostly used as a first qualitative test before the use of more sophisticated interferometric techniques.

One of the main advantages of the Foucault test is its easy interpretation from the geometrical point of view [1–3], which states that the transverse ray aberrations are functions of the partial derivatives of the wavefront. The geometrical theory has been widely used to evaluate large aberrations.

The first advances in the analysis from the point of view of the physical theory were reported by Gascoigne [4] and Linfoot [5–8]. Later, some other advances were reported by Barakat [9], Welford [10], Katzoff [11], and Wilson [12]; in particular, Katzoff [11] proposed an inversion method of Linfoot's formula using a linear approximation that permits one to obtain an expression of the wavefront error in terms of the irradiance distribution. Unfortunately, the physical theory has been mostly used to analyze the complex amplitude and the irradiance in the image plane considering the particular case of wavefront errors smaller than the wavelength.

Opticians have long used the Foucault test in the geometrical sense; however, the interpretation of the test from the physical theory has been almost discarded for most practical purposes.

Despite its great potential, the Foucault test has been little explored for use as a sophisticated technique for quantitative evaluations. Although the geometrical sense has been widely used to analyze the Foucault test, it has some limitations for this purpose. For this reason it is necessary to explore in depth the physical theory to overcome these limitations and to develop more sophisticated quantitative evaluation techniques using the Foucault test, which is part of our the current research.

In order to show a more precise interpretation from the physical theory and its application to quantitative evaluations, we now derive irradiance distribution models that are obtained in closed form. As will be shown, the models are deduced in this way using some properties of the Hilbert transform.

## 2. PHYSICAL THEORY OF THE FOUCAULT TEST

Consider the basic Foucault arrangement to test spherical mirrors, as depicted in Fig. 1.

For simplicity, if we assume uniform illumination the complex amplitude of the aberrated wavefront coming from the mirror can be defined as

$$\psi_o(x, y) = a(x, y)e^{i\frac{2\pi}{\lambda}W(x, y)}, \quad (1)$$

where  $i = \sqrt{-1}$ ,  $\lambda$  is the wavelength of the light,  $W(x, y)$  the wavefront deformations measured with respect to a reference sphere, and the exit pupil of the system defined by its radius  $r_p$  such that

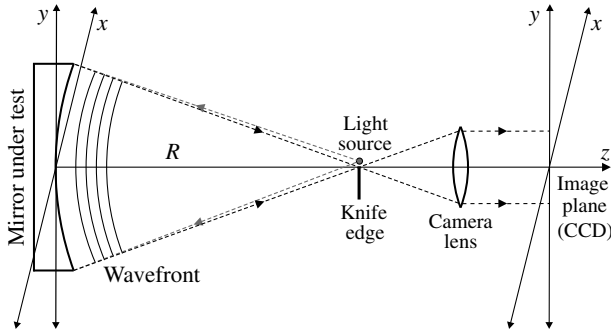


Fig. 1. The Foucault test for a spherical mirror.

$$a(x, y) = a_o \times \text{circ}\left(\frac{r}{r_p}\right), \tag{2}$$

where

$$\text{circ}\left(\frac{r}{r_p}\right) = \begin{cases} 1 & \text{if } r \leq r_p \\ 0 & \text{otherwise} \end{cases}, \tag{3}$$

$a_o$  is a constant, and  $r = \sqrt{x^2 + y^2}$ . To find the complex amplitude  $\psi_i(x, y)$  in the image plane, we can consider a linear space-invariant system  $h(x, y)$  such that

$$\begin{aligned} \psi_i(x, y) &= \int_{-\infty}^{\infty} \int_{-\infty}^{\infty} \psi_o(x', y') h(x - x', y - y') dx' dy' \\ &= \psi_o(x, y) * h(x, y), \end{aligned} \tag{4}$$

where  $*$  represents convolution. Then, using the convolution theorem,  $\psi_i(x, y)$  can also be represented by means of the inverse Fourier transform as [3]

$$\begin{aligned} \psi_i(x, y) &= \int_{-\infty}^{\infty} \int_{-\infty}^{\infty} H(u, v) \Psi_o(u, v) e^{i2\pi(xu + yv)} du dv \\ &= \mathcal{F}^{-1}\{H(u, v) \Psi_o(u, v)\}, \end{aligned} \tag{5}$$

where  $H$  and  $\Psi_o$  represent the Fourier transforms of  $h$  and  $\psi_o$ , respectively, being

$$u = \frac{x}{\lambda R} \quad \text{and} \quad v = \frac{y}{\lambda R}. \tag{6}$$

In Eq. (6)  $R$  represents the radius of the reference sphere.

The knife edge is a filter in the Fourier plane blocking out part of the converging light. If it is placed vertically coinciding with the  $v$  axis it can be represented by the Heaviside unit step function:

$$\begin{aligned} H(u, v) &= \begin{cases} 0 & \text{if } u < 0 \\ \frac{1}{2} & \text{if } u = 0 \\ 1 & \text{if } u > 0 \end{cases} \\ &= H(u) \\ &= \frac{1}{2}(1 + \text{sgn}(u)). \end{aligned} \tag{7}$$

As can be seen,  $H(u, v)$  is also expressed in terms of the signum function. Since the filtering is realized only along the  $u$  axis, it is represented as a single one-dimensional

function parameterizing the  $v$  variable. Now, substituting Eq. (7) in Eq. (5) we obtain

$$\begin{aligned} \psi_i(x, y) &= \frac{1}{2}(\psi_o(x, y) + \mathcal{F}^{-1}\{\text{sgn}(u)\Psi_o(u, v)\}) \\ &= \frac{1}{2}(\psi_o(x, y) + i\mathcal{H}\{\psi_o(x, y)\}) \\ &= \frac{1}{2}\left(\psi_o(x, y) + \frac{i}{\pi} \int_{-\infty}^{\infty} \frac{\psi_o(x', y)}{x' - x} dx'\right), \end{aligned} \tag{8}$$

where  $\mathcal{H}$  represents the Hilbert transform operator with respect to  $x$ . When the mirror is free of aberrations, the Hilbert transform in Eq. (8) results in the well-known form

$$\mathcal{H}\{\psi_o(x, y)\} = \frac{1}{\pi} \ln \left| \frac{x + \sqrt{r_p^2 - y^2}}{x - \sqrt{r_p^2 - y^2}} \right|, \tag{9}$$

which, in terms of intensity, represents a brilliant ring of light at the edge commonly observed in experiments.

### 3. SHADOWGRAM MODELING FROM THE PHYSICAL THEORY

As can be seen, the analysis of the second term in Eq. (8) is the key to deriving an expression for  $u_i(x, y)$ , so we shall first establish a result concerning such term.

The Hilbert transform is a useful mathematical tool to construct an analytic function  $\hat{g}(x)$  from a real function  $g(x)$ , the two being associated in the following way:

$$\hat{g}(x) = g(x) - i\mathcal{H}\{g(x)\}, \tag{10}$$

where  $g(x)$  and  $\mathcal{H}\{g(x)\}$  are the real and imaginary parts of  $\hat{g}(x)$ , respectively. The Hilbert transform is also usually referred to as the quadrature function of  $g(x)$ .

For simplicity in the following derivation we assume that  $r_p$  is large enough that the size of the Airy disc is much smaller than the spectral lobe due to  $W$ . Then, taking into account that  $\psi_o(x, y)$  represents an analytic signal, we now use some properties of the Hilbert transform [13] to obtain an expression for  $\mathcal{H}\{\psi_o(x, y)\}$ , in particular for the case

$$W_x(x, y) = \frac{\partial W}{\partial x} > 0, \quad \forall x. \tag{11}$$

Considering that we can express  $\psi_o$  as

$$\psi_o(x, y) = \alpha(x, y) + i\beta(x, y), \tag{12}$$

where  $\alpha$  and  $\beta$  represent the real and imaginary parts of  $\psi_o$ , respectively, then

$$\begin{aligned} \mathcal{H}\{\psi_o(x, y)\} &= \mathcal{H}\{\alpha(x, y)\} + i\mathcal{H}\{\beta(x, y)\} \\ &= \beta(x, y) + i\mathcal{H}\{\mathcal{H}\{\alpha(x, y)\}\} \\ &= \beta(x, y) - i\alpha(x, y) \\ &= -i\psi_o(x, y). \end{aligned} \tag{13}$$

Generally, the condition of Eq. (10) is not satisfied (i.e.,  $W$  is not a monotonically increasing function for  $x$ ). In a similar way, it can also be verified that  $\mathcal{H}\{\psi_o(x, y)\} = +i\psi_o(x, y)$

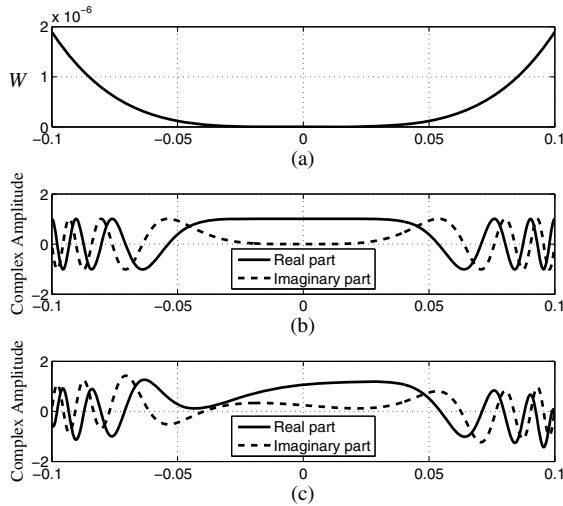


Fig. 2. The horizontal axis represents the  $x$  variable in meters for  $y = 0$ . (a) Profile of a simulated wavefront. (b) The normalized complex amplitude  $\psi_o$ . (c) The normalized complex amplitude  $i\mathcal{H}\{\psi_o\}$ . Note the sign inversion with respect to  $\psi_o$  for  $W_x < 0$ .

for the case  $W_x(x, y) < 0, \forall x$ . As a consequence of the Hilbert transform properties (i.e., it represents the quadrature of the function  $\psi_o$ ) the local sign of  $W_x$  determines the sign of Eq. (13) (see Fig. 2).

Therefore, in general

$$\mathcal{H}\{\psi_o(x, y)\} \approx -i\text{sgn}(W_x)\psi_o(x, y). \quad (14)$$

Then, we rewrite Eq. (8) as

$$\begin{aligned} \psi_i(x, y) &\approx \frac{1}{2}[\psi_o(x, y) + \text{sgn}(W_x)\psi_o(x, y)] \\ &\approx H(W_x)\psi_o(x, y). \end{aligned} \quad (15)$$

Finally, the irradiance  $I(x, y)$  that represents the shadowgram can be modeled as

$$I(x, y) \approx H(W_x)a^2(x, y). \quad (16)$$

Since Eq. (14) is not well defined for  $W_x \simeq 0$ , Eq. (16) is an approximation to  $I(x, y)$ , so that we can see in real experiments that the shadowing is gradual instead of occurring a sharp edge. This can be explained from the fact that

$$\begin{aligned} \Psi_o(u, v) &= a_0\mathcal{F}\{\text{circ}(r/r_p)\} * \mathcal{F}\{e^{i\frac{2\pi}{\lambda}W(x,y)}\} \\ &= a_0r_p \frac{J_1(2\pi r_p \rho)}{\rho} * \mathcal{F}\{e^{i\frac{2\pi}{\lambda}W(x,y)}\}, \end{aligned} \quad (17)$$

where  $\rho = \sqrt{u^2 + v^2}$ , which means that for  $r_p$  large

$$\Psi_o(u, v) \approx a_0\mathcal{F}\{e^{i\frac{2\pi}{\lambda}W(x,y)}\}. \quad (18)$$

In other words, the shadowing in the image becomes sharper with a larger  $r_p$ .

#### 4. QUANTITATIVE ANALYSIS FROM THE PHYSICAL THEORY

A quantitative method to detect  $W_x$  at a given point  $(x, y)$  is to record the intensity as a function of the knife-edge position  $x_s$  as indicated in Fig. 3; then the edge in the plot of intensity versus the knife-edge position is used to determine  $W_x$  [1,2].

Using the dummy variable  $\hat{u} = u - u_s$ , where  $u_s = x_s/(\lambda R)$ , the complex amplitude as a function of  $x_s$  in the image plane is

$$\begin{aligned} \psi_i(x, y; x_s) &\approx \frac{1}{2}\mathcal{F}^{-1}\{[1 + \text{sgn}(\hat{u})]\Psi_o(\hat{u} + u_s, v)\} \\ &\approx \frac{1}{2}(\psi_o(x, y)e^{i2\pi x u_s} + i\mathcal{H}\{\psi_o(x, y)e^{i2\pi x u_s}\}) \\ &\approx H(W_x + \lambda u_s)\psi_o(x, y)e^{i2\pi x u_s}, \end{aligned} \quad (19)$$

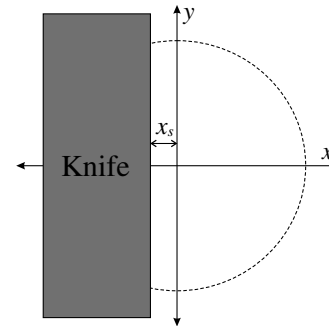


Fig. 3. Displacement  $x_s$  of the knife edge for quantitative evaluations.

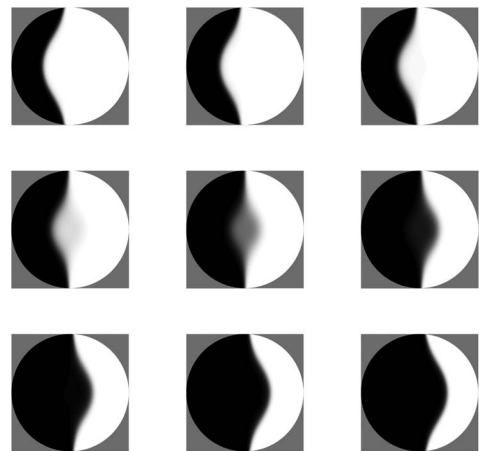


Fig. 4. Simulation of a sequence of shadowgrams (from left-top to right-bottom) for several positions ( $x_s$ ) of the knife edge, using a mirror with spherical aberration.

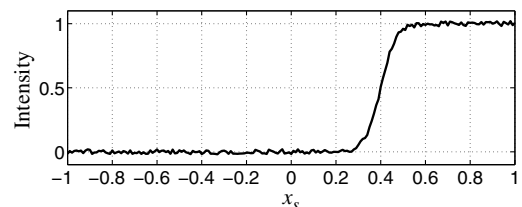


Fig. 5. Simulation of a typical normalized  $I - x_s$  graph of a given site  $(x, y)$  in the sequence of shadowgrams.

and the intensity of the Foucault pattern as a function of  $x_s$  is then modeled as

$$I(x, y; x_s) \approx H(W_x + x_s/R)a^2(x, y). \quad (20)$$

The edge in the  $I - x_s$  graph at a given site  $(x, y)$  occurs for  $H(0)$ , that is, where  $W_x = -x_s/R$  (see Figs. 4 and 5).

## 5. CONCLUSIONS

We have derived expressions to model the irradiance of shadowgrams using the physical theory, which allows a more precise interpretation from this point of view. The signum function that represents the knife edge in the Fourier plane permits expression of the complex amplitude in the image plane in terms of the Hilbert transform. As shown, the use of some basic properties of this transform has been the key to deriving such image models. From this point of view we have also described a methodology for the quantitative analysis of the test.

## ACKNOWLEDGMENTS

The authors wish to acknowledge the partial support for the realization of this work by the Consejo Zacatecano de Ciencia y Tecnología (COZCYT), through the project ZAC-2013-C02-203103, and the Consejo Nacional de Ciencia y Tecnología (CONACYT) of México for the scholarship of Gustavo Rodríguez.

## REFERENCES

1. E. M. Granger, "Wave-front measurements from a knife-edge test," *Proc. SPIE* **429**, 174–177 (1983).
2. D. E. Vandenberg, W. D. Humbel, and A. Wertheimer, "Quantitative evaluation of optical surfaces by means of an improved Foucault test approach," *Opt. Eng.* **32**, 1951–1954 (1993).
3. D. Malacara, *Optical Shop Testing*, 3rd ed. (Wiley-Interscience, 2007), Chap. 8.
4. S. C. B. Gascoigne, "The theory of the Foucault test," *Mon. Not. R. Astron. Soc.* **104**, 326–334 (1944).
5. E. H. Linfoot, "Astigmatism under the Foucault test," *Mon. Not. R. Astron. Soc.* **105**, 193–199 (1945).
6. E. H. Linfoot, "A contribution to the theory of the Foucault test," *Proc. R. Soc. A* **186**, 72–99 (1946).
7. E. H. Linfoot, "On the interpretation of the Foucault test," *Proc. R. Soc. A* **193**, 248–259 (1948).
8. E. H. Linfoot, "The Foucault test," in *Recent Advances in Optics* (Oxford, 1958), Chap. II, pp. 128–174.
9. R. Barabak, "General diffraction theory of optical aberration tests, from the point of view of spatial filtering," *J. Opt. Soc. Am.* **59**, 1432–1439 (1969).
10. W. T. Welford, "A note on the theory of the Foucault knife-edge test," *Opt. Commun.* **1**, 443–445 (1970).
11. S. Katzoff, "Quantitative determination of optical imperfections by mathematical analysis of the Foucault knife-edge test pattern," NASA Tech. Note D-6119 (NASA, August 1971).
12. R. G. Wilson, "Wavefront-error evaluation by mathematical analysis of experimental Foucault-test data," *Appl. Opt.* **14**, 2286–2297 (1975).
13. F. W. King, *Hilbert Transforms*, Vol. 1–2 of *Encyclopedia of Mathematics and Applications* (Cambridge University, 2009), pp. 145–251.